© Indian Academy of Sciences

An investigation of variable viscosity Carreau fluid and mixed convective stagnation point flow

MEHBOOB ALI[1,2,*], FAISAL SULTAN[5], MUHAMMAD SHAHZAD[2], ARSHED ALI[3],
SYED INAYAT ALI SHAH[3] and MOHAMED ALTANJI[4]

[1]Department of Mathematics and Statistics, Hazara University, Mansehra, Pakistan
[2]Department of Mathematics and Statistics, University of Haripur, Haripur 22620, Pakistan
[3]Department of Mathematics, Islamia College Peshawar, Peshawar 25120, Pakistan
[4]Department of Mathematics, College of Science, King Khalid University, Abha 61413, Saudi Arabia
[5]Department of Mathematics, Khwaja Fareed University of Engineering & Information Technology, Rahim Yar Khan, Pakistan
*Corresponding author. E-mail: mehboob_maths@hu.edu.pk

Abstract.   Here, our aim is to investigate incompressible Carreau fluid with variable properties and nanoparticles are considered to improve the heat transfer. This communication also highlights the thermal significances of Joule heating and incorporation of activation energy. The mathematical modelling is constructed for physical phenomena by assuming boundary layer problems. The well-known numerical treatment Bvp4c is utilised to solve the nonlinear problem and transform the governing equations. The effects of different physical parameters are assessed graphically and numerical data of skin friction and Nusselt number are explored. It is noted that activation energy rate improves and it decreases with the exponential fitted rate on concentration profile. The simulations for the current model reveal that the Nusselt number decreases with increasing exponential fitted rate and elastic deformation while for activation it increases.

1. Introduction

Rapid advancement in nanotechnology with potential heat transport features has been communicated by many researchers in recent years. Nanofluids are a class of fluids that are formed by adding nanosized materials in base fluids. The scattered solid particles in the base fluid enhance thermophysical properties and conserve important properties like thermal resistance, heat exchanger functioning, cooling of nuclear reactors, etc. Choi [1] first introduced the concept of increasing the thermal conductance of the base fluids by adding nanoparticles. Khan *et al* [2] reported the activation and chemical reaction of the cross nanofluid. Sultan *et al* [3] theoretically studied the thermophoresis and Brownian motion of the cross fluid. Abbas *et al* [4] considered a mathematical model for the cross nanofluid flow with entropy

generation. Ali *et al* [5] investigated thermal radiative and non-uniform source on Sisko nanofluid in the presence of Lorentz forces on a curved surface. Khan *et al* [6] studied numerical simulation of the Casson nanofluid over heated surface. Feature of magnetic field and nanofluid over a stretching sheet are reported by Ganga *et al* [7]. Hakeem *et al* [8] analysed the non-uniform heat source/sink and MHD flow of a nanofluid over a stretching sheet. Govindaraju *et al* [9] introduced nanofluid over a stretching sheet with Lorentz forces and heat source/sink. Hakeem *et al* [10] designed hydromagnetic flow of the Buongiorno model nanofluid through a vertical plate.

Non-Newtonian fluids are very important in modern sciences which include industrial and mechanical fields. These types of fluids do not follow Newton's viscosity law. They include ketchup, blood, yogurt, toothpaste,

paints, etc. Therefore, Navier–Stokes statements are not enough to indicate the behaviour of such types of materials due to their complex nature. Many researchers [11–21] presented non-Newtonian models. Nowadays, viscoelastic fluids are commonly used in the movement of biological fluids, bioengineering, paint production, plastic films, pharmaceuticals, extrusion, drawing sheet, solution suspension and several other production processes. Various important applications of convective thermal transport which include nuclear reactors, solar collectors, aeronautics, heating and cooling devices, many other experimental and theoretical investigations on the buoyant movement of different fluids in various geometries have been investigated [22–24].

This communication presents a discussion about the physical properties of nanoparticle with variable properties over a starching sheet. The Carreau fluid is assumed to be a base fluid. The shear-thinning nature of the Carreau fluid is more affected. Studies by many researchers concerning new developments in different fluid flow models are listed in refs [25–28]. The applications of the base fluid are mostly referred to lubricating oil production.

2. Formulation

In this computational model, we consider the convective flow of steady Carreau fluid by continuously starched surface near the stagnation point under the influence of nanoparticles. The direction of flow on a stretchable surface is in such a manner that the x-axis is along the surface of the sheet and the y-axis is orthogonal to the flow. An incompressible flow is confined to $y > 0$. Also, thermophysical features of the fluid at the surface are taken as variables. The constitutive relation for a Carreau material is

$$\frac{\partial u}{\partial y} + \frac{\partial v}{\partial x} = 0. \tag{1}$$

Momentum equation:

$$u\frac{\partial u}{\partial x} + v\frac{\partial u}{\partial y} = \frac{1}{\rho}\frac{\partial}{\partial y}\left[\eta_0\left[1 + \lambda^2\left(\frac{\partial u}{\partial y}\right)^2\right]^{\frac{n-1}{2}}\left(\frac{\partial u}{\partial y}\right)\right]$$
$$+ u_e\frac{\mathrm{d}u_e}{\mathrm{d}x} + g\beta_T\left(T - T_\infty\right). \tag{2}$$

Energy equation:

$$u\frac{\partial T}{\partial x} + v\frac{\partial T}{\partial y} = \frac{1}{\rho c_p}\frac{\partial}{\partial y}\left(K(T)\frac{\partial T}{\partial y}\right)$$
$$+ \tau\left[D_B\left(\frac{\partial C}{\partial y}\frac{\partial T}{\partial y}\right) + \frac{D_T}{T_\infty}\left(\frac{\partial T}{\partial y}\right)^2\right]. \tag{3}$$

Concentration:

$$u\frac{\partial C}{\partial x} + v\frac{\partial C}{\partial y} = \frac{1}{\rho c_p}\frac{\partial}{\partial y}\left(D(C)\frac{\partial C}{\partial y}\right)$$
$$+ D_B\frac{\partial^2 C}{\partial y^2} + \frac{D_T}{T_\infty}\frac{\partial^2 T}{\partial y^2}$$
$$- k_c^2\left(C - C_\infty\right)\left(\frac{T}{T_\infty}\right)^m$$
$$\times \exp\left(-\frac{E_a}{KT}\right). \tag{4}$$

Boundary conditions:

$$u = u_w(x) = cx, \quad v = v_w, \quad -K(T)\frac{\partial T}{\partial y} = (T - T_w),$$
$$D_B\frac{\partial C}{\partial y} + \frac{D_T}{T_\infty}\frac{\partial T}{\partial y} = 0 \quad \text{at } y = 0, \tag{5}$$
$$u \to u_e = ax, \quad T \to T_\infty, \quad C \to C_\infty \quad \text{as } y \to \infty, \tag{6}$$

where

$$K(T) = k_\infty\left(1 + \varepsilon_1\frac{T - T_\infty}{\Delta T}\right),$$
$$D(C) = D_\infty\left(1 + \varepsilon_2\frac{C - C_\infty}{\Delta C}\right), \tag{7}$$
$$\frac{1}{\mu} = \frac{1}{\mu_\infty}\left[1 + \gamma_1\left(T - T_\infty\right)\right], \tag{8}$$

This equation can be rewritten as

$$\frac{1}{\mu} = \alpha(T - T_\Gamma). \tag{9}$$

Consider

$$\Psi = x\sqrt{cv}f(\eta), \quad u = cxf'(\eta), \quad v = -\sqrt{cv}f(\eta),$$
$$\theta(\eta) = \frac{T - T_\infty}{T_w - T_\infty}, \quad \phi(\eta) = \frac{C - C_\infty}{C_w - C_\infty}, \quad \eta = y\sqrt{\frac{c}{v}}. \tag{10}$$

Equation (1) holds while eqs (2) and (6) become

$$f'''\left[1 + \left(Wef''\right)^2\right]^{\frac{n-3}{2}}\left[1 + n(Wef'')^2\right]$$
$$+ \left(\frac{\theta'}{\theta_r - \theta}\right)f''\left[1 + (Wef'')^2\right]^{\frac{n-1}{2}}$$
$$+ \left(\frac{\theta_r - \theta}{\theta_r}\right)\left[ff'' - \left(f'\right)^2 + G\theta + A^2\right] = 0, \tag{11}$$
$$(1 + \varepsilon_1\theta)\theta'' + \varepsilon_1\left(\theta'\right)^2 + P_rN_b\theta'\phi' + P_rN_t\theta'^2$$
$$+ P_r\left[f\theta' - f'\theta\right] = 0, \tag{12}$$
$$(1 + \varepsilon_2\phi)\phi'' + \varepsilon_2\phi'^2 + \frac{N_t}{N_b}\theta'' + Sc\left[f\phi' - f'\phi\right]$$

$$- Sc\sigma \, (1 + \delta\theta)^m \, \phi \exp\left(-\frac{E}{1 + \delta\theta}\right) = 0. \qquad (13)$$

Boundary conditions are

$$f = s, \quad f' = 1, \quad \theta' = -\gamma(1 - \theta),$$
$$N_b\phi' + N_t\theta' = 0 \quad \text{at } \eta = 0, \qquad (14)$$
$$f' = A, \quad \theta = 0, \quad \phi' = 0 \quad \text{as } \eta \to \infty. \qquad (15)$$

Involved physical parameters are

$$We = \frac{\lambda^2 x^2 c^3}{\upsilon}, \quad s = -\frac{v_w}{\sqrt{cv}}, \quad P_r = \frac{\upsilon}{\alpha},$$

$$\theta_r = \frac{T_r - T_\infty}{T_w - T_\infty} = -\frac{1}{\gamma(T_w - T_\infty)},$$

$$G = \frac{Gr_x}{Re^2 x} = \frac{g\beta_T b}{c^2}, \quad N_t = \frac{\tau D_T(T_w - T_\infty)}{\upsilon T_\infty},$$

$$Gr_x = \frac{g\beta_T(T_w - T_\infty)x^3}{v^2}, \quad Re_x = \frac{u_w(x)x}{\upsilon},$$

$$N_b = \frac{\tau D_B (C_w - C_\infty)}{\upsilon}, \quad A = \frac{a}{c}, \quad \sigma = \frac{k_c^2}{a},$$

$$E = \frac{E_a}{k_\infty T_\infty}, \quad \delta = \frac{T_w - T_\infty}{T_\infty}. \qquad (16)$$

Non-dimensional skin friction C_f and local Nusselt number Nu_x become

$$\frac{1}{2}C_f Re_x^{\frac{1}{2}} = \left(\frac{\theta_r}{\theta_r - \theta}\right)\left[1 + (We f''(0))^2\right]^{\frac{n-1}{2}} f''(0), \qquad (17)$$

$$Re_x^{-\frac{1}{2}} Nu_x = -\left(1 + \frac{4}{3}N\right)\theta'(0). \qquad (18)$$

3. Solution of the proposed problem

The ruling governed system of first-order ODEs for the flow field is solved by utilising the MATLAB tool bvp4c technique. The bvp4c technique is applied for first-order initial boundary value problems. Thus, we have used the bvp4c technique which controls the convergences of the dimensional parameter.

4. Analysis

The main aim of this paper is to investigate the variation of dimensionless parameters of flow, temperature and concentration field. The velocity components $(f'(\eta))$, temperature $(\theta(\eta))$ and concentration field $(\phi(\eta))$ of the fluid are examined in figures 1–14. Figures 1–4 show the variation in velocity field $(f'(\eta))$, due to an increase in A, G, s and We. Figure 1 displays the variation of velocity with A, the ratio of rate constant. The
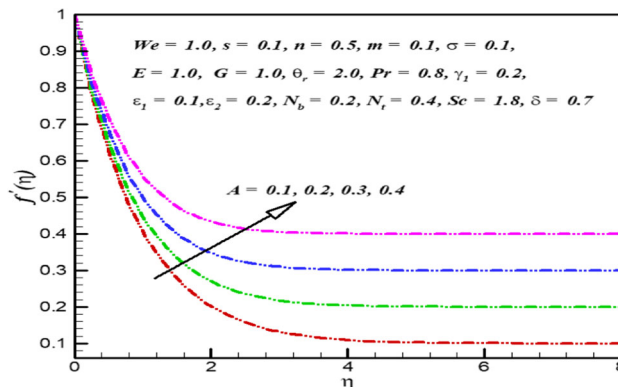

Figure 1. Influence of A on velocity $(f'(\eta))$.

Figure 2. Influence of G on velocity $(f'(\eta))$.
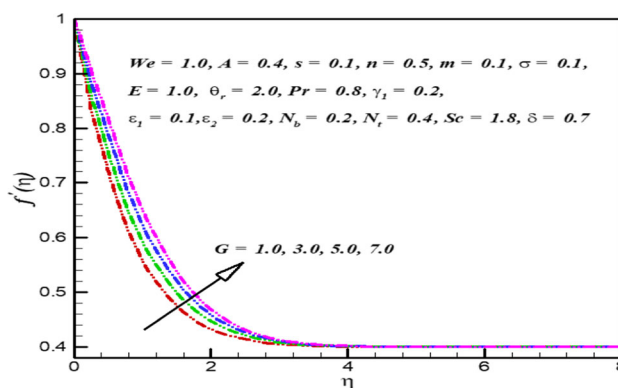

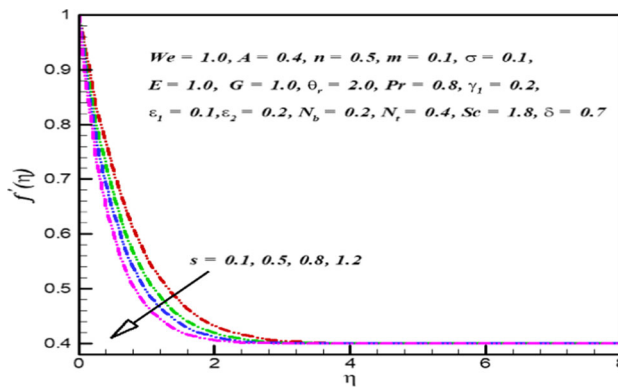**Figure 3.** Influence of s on velocity $(f'(\eta))$.

boundary layer thickness is stronger for $A < 1$ and starching rate controls the free stream rate. Similarly, for $A > 1$ the boundary layer thickness is reduced while velocity field $(f'(\eta))$ increases. The effect of mixed convection parameter (G) on the velocity field is explored in figure 2. Here, we observe that when mixed convection parameter (G) increases, velocity field $(f'(\eta))$ increases. Buoyancy forces occur when the mixed convection parameter due to velocity $(f'(\eta))$ increases. Figure 3 illustrates the influence of section parameter (s)
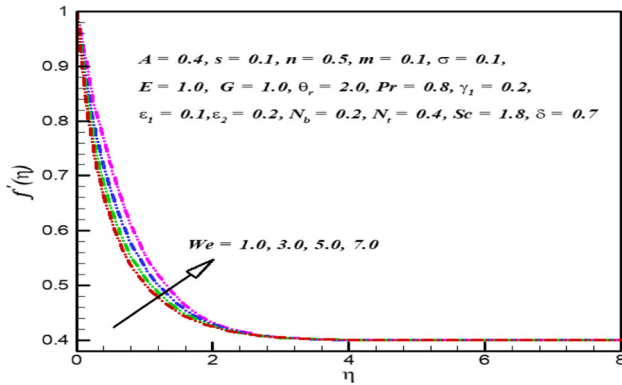
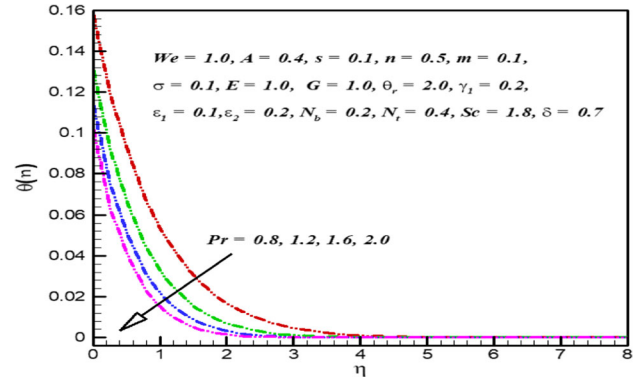**Figure 4.** Influence of *We* on velocity ($f'(\eta)$).

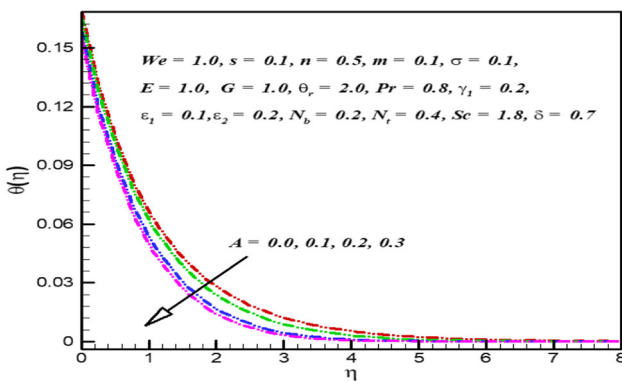**Figure 5.** Influence of *A* on temperature ($\theta(\eta)$).

Figure 6. Influence of ε_1 on temperature ($\theta(\eta)$).
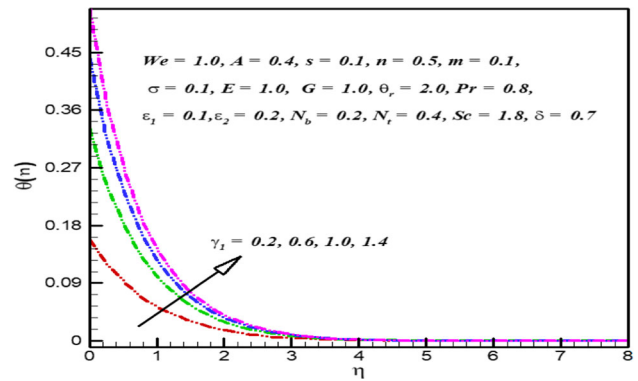

Figure 7. Influence of *Pr* on temperature ($\theta(\eta)$).
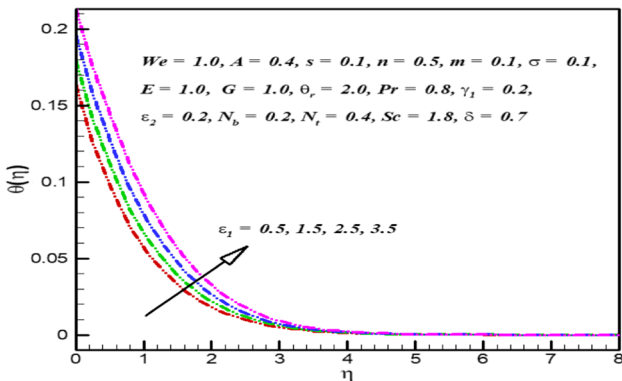

Figure 8. Influence of γ_1 on temperature ($\theta(\eta)$).
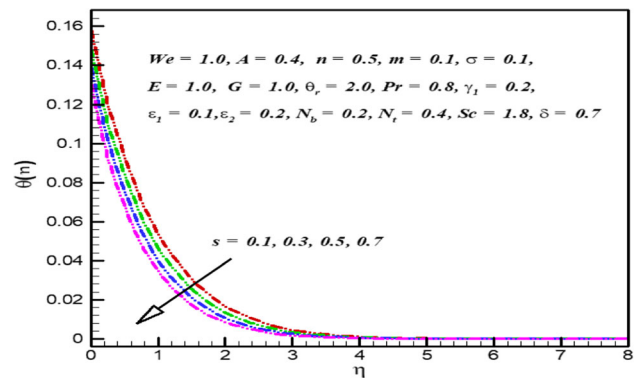

Figure 9. Influence of *s* on temperature ($\theta(\eta)$).

on velocity field ($f'(\eta)$). The fluid particle is sucked by the starching sheet because of some resistances occurring in fluid flow and then velocity decreases. The impact of local Weissenberg number *We* on velocity field ($f'(\eta)$) is shown in figure 4. Figures 5–9 indicate variation in temperature field ($\theta(\eta)$). Figure 5 shows the effect of *A* on the temperature field ($\theta(\eta)$). Temperature field ($\theta(\eta)$) decreases for increasing values of *A*. Physically, by increasing the value of *A*, more pressure is produced which gives less resistance to the fluid. Figure 6 demonstrates the influence of variable conductivity

(ε_1) on the temperature field ($\theta(\eta)$). This figure shows that increasing the values of variable conductivity (ε_1) enhances the temperature field ($\theta(\eta)$). The influence of *Pr* on the temperature field ($\theta(\eta)$) is displayed in figure 7. Figure 7 shows that increase *Pr* tends to decrease the temperature field ($\theta(\eta)$). Temperature field declines as *Pr* strengthens. This is the reason for the reduction in thermal conductivity of the fluid with increasing *Pr*. The temperature field ($\theta(\eta)$) is sketched in figure 8 for increasing values of generalised Biot number (γ). This figure shows that temperature field ($\theta(\eta)$) decreases
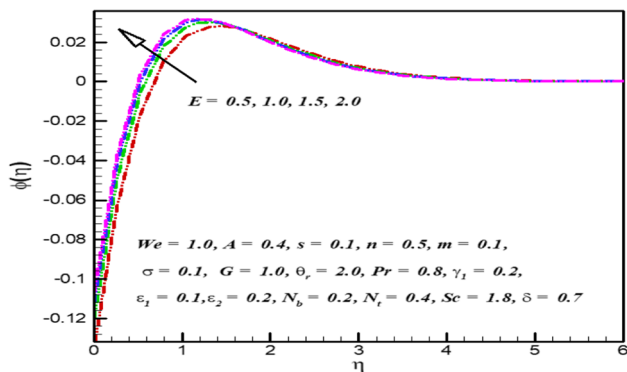
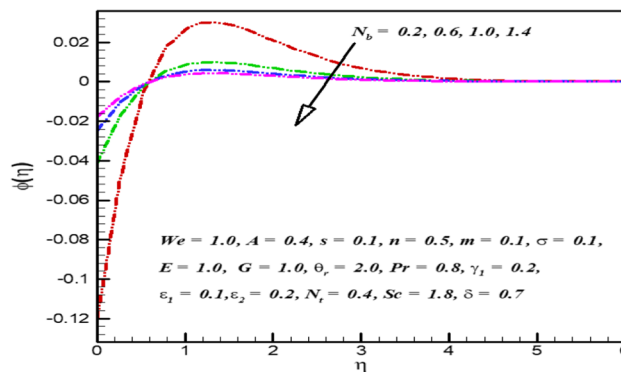**Figure 10.** Influence of E on concentration ($\phi(\eta)$).
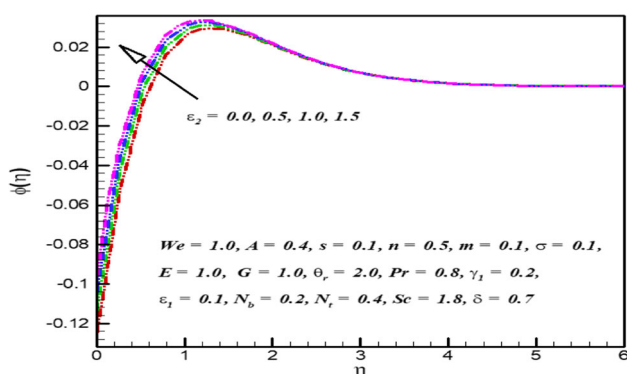

Figure 12. Influence of N_b on concentration ($\phi(\eta)$).

Figure 11. Influence of ε_2 on concentration ($\phi(\eta)$).

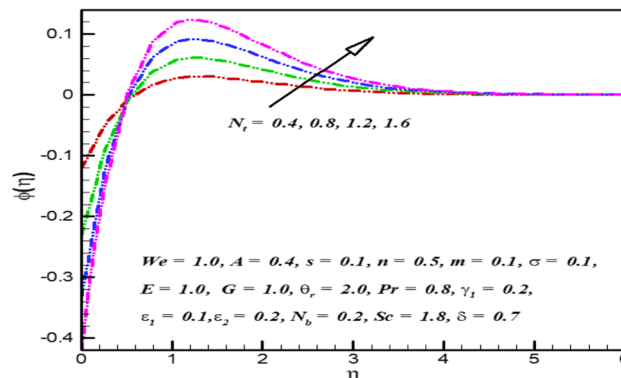**Figure 13.** Influence of N_t on concentration ($\phi(\eta)$).

Figure 14. Influence of Sc on concentration ($\phi(\eta)$).

for increasing values of generalised Biot number (γ_1). Physically, less resistance from the thermal wall causes augmentation in convective heat transfer to the fluid. Figure 9 explores the deviation of section parameter (s) on the temperature field ($\theta(\eta)$). Here, temperature field ($\theta(\eta)$) decreases for increasing section parameter (s). Physically, the liquid particle observes the stretching sheet and each particle transfers energy to the environment. Figures 10–13 indicate variation in concentration field ($\phi(\eta)$). Figure 10 shows the effect of activation energy (E) on concentration field ($\phi(\eta)$). It can be seen that the concentration field ($\phi(\eta)$) is increasing with an increment in activation energy (E). We have detected that higher activation energy and temperature reduce the reaction rate because the reaction mechanism is reduced. Thus, the concentration field increases for the activation energy. Figure 11 shows the variation in temperature of the Carreau nanofluid with variable conductivity (ε_2). Graphical data show that the Carreau nanofluid temperature increases with increasing ε_2. Figure 12 is plotted to investigate the Brownian motion parameter (N_b) on concentration field ($\phi(\eta)$). Here, we detect that increasing the values of thermophoresis parameter (N_t) decreases the concentration field ($\phi(\eta)$). Figure 14 is plotted to show the effect of Schmidt number (Sc) on

($\theta(\eta)$). Here is a decreasing function for larger Schmidt number (Sc).

Table 1 shows how much order of computation is required for convergent solution. Table 1 shows that the present solutions are in excellent agreement with other previously published data. Table 2 examines the skin friction ($\frac{1}{2}Re^{1/2}C_{fx}$) and Nusselt number ($Re^{-1/2}Nu_x$) for dimensionless parameters A, N, G and θ_r. Table 2 shows that the skin friction becomes less for increasing parameter A while the opposite occurs for N, G and θ_r. Similarly, the rate of heat transport

Table 1. Comparison of the current results of $f''(0)$ with previous results [29] and [30] for different values of A when $n = 1.0$, and $S = 0.0 = \lambda_1 = G = \theta_r$.

A	Ref. [29]	Ref. [30]	Present
0.01	−0.998024	−0.9963	−0.998025
0.02	−0.995783	−0.9930	−0.995782
0.05	−0.987580	−0.9830	−0.987583
0.10	−0.969386	−0.9603	−0.969384
0.50	−0.918107	−0.9080	−0.918109
0.20	−0.667260	−0.6605	−0.667261
1.00	0.000000	0.0000	0.000000
2.00	2.01767	2.0181	2.01762
3.00	4.72964		4.72967

Table 2. Numerical outcomes $\frac{1}{2}Re^{1/2}C_{fx}$ for various physical parameters with $n = 0.8$.

A	N	G	θ_r	$\frac{1}{2}Re^{1/2}C_{fx}$m	$Re^{-1/2}Nu_x$
0.3	0.1	1.0	0.1	−0.351696	0.190901
0.5	–	–	–	−0.290545	0.192431
0.8	–	–	–	−0.129130	0.194374
	0.5	–	–	−0.348124	0.271452
–	0.8	–	–	−0.345572	0.329765
–	0.9	–	–	−0.344750	0.348872
–	–	1.2	–	−0.347400	0.190969
–	–	1.6	–	−0.338703	0.191099
–	–	2.0	–	−0.329868	0.191223
–	–	–	2.2	−0.350188	0.190888
–	–	–	2.6	−0.347888	0.190868
–	–	–	3.0	−0.346216	0.190853

increases for increasing values of dimensionless parameters A, N and G. However, opposite behaviour is observed for θ_r.

5. Main outcomes

Carreau flow of nanomaterial and variable properties are examined in the present analysis. Heat and mass transport via convection and activation energy are studied, respectively. The main theme of this study is to control the flow of fluid, skin friction using heat and mass transport rate. The velocity of fluid ($f'(\eta)$) is increased by increasing the values of A. Section parameter (s) decay is observed in the component of velocity field ($f'(\eta)$). Increase in mixed convection parameter (G) increases velocity ($f'(\eta)$). The fluid concentration ($\phi(\eta)$) decreases for increasing values of Brownian motion parameter (N_b). The concentration of Carreau nanofluid decreases with increasing values of Sc. The augmentation in activation energy parameter (E) corresponds to a higher concentration ($\phi(\eta)$). Skin friction decreases with increasing values of A, N, G and θ_r.

Heat transfer rate increases with increasing values of A, N, G and θ_r.

References

[1] S U S Choi and A Jeffrey, Enhancing thermal conductivity of fluids with nanoparticles, No. ANL/MSD/CP-84938; CONF-951135-29 (Argonne National Lab, Argonne, IL, USA, 1995)

[2] W A Khan, F Sultan, M Ali, M Shahzad, M Khan and M Irfan, *J. Braz. Soc. Mech. Sci. Eng.* **41**, 4 (2019), https://doi.org/10.1007/s40430-018-1482-0

[3] F Sultan, W A Khan, M Ali, M Shahzad, M Irfan and M Khan, *Pramana – J. Phys.* **92**, 21 (2019), https://doi.org/10.1007/s12043-018-1676-0

[4] S Z Abbas, W A Khan, H Sun, M Ali, M Irfan, M Shahzed and F Sultan, *Appl. Nanosci.* **10**, 3149 (2020), https://doi.org/10.1007/s13204-019-01039-9

[5] M Ali, W A Khan, F Sultan and M Shahzad, *Physica A* **550**, 124012 (2020), https://doi.org/10.1016/j.physa.2019.124012

[6] S Khan, W Shu, M Ali, F Sultan and M Shahzad, *Appl. Nanosci.* **10**, 5391 (2020), https://doi.org/10.1007/s13204-020-01546-0

[7] B Ganga, M Govindaraju and A K Abdul Hakeem, *Iran. J. Sci. Technol. Trans. Mech. Eng.* **43**, 707 (2019), https://doi.org/10.1007/s40997-018-0227-0

[8] A K Abdul Hakeem, M Govindaraju, B Ganga and M Kayalvizhi, *Sci. Iran. Trans. F* **23(3)**, 1524 (2016)

[9] M Govindaraju, B Ganga and A K Abdul Hakeem, *Front. Heat Mass Transf.* **8**, 10 (2017)

[10] A K Abdul Hakeem, B Ganga, S Mohamed Yusuff Ansari and N Vishnu Ganesh, *J. Heat Mass Transf. Res.* **3(2)**, 153 (2016)

[11] M K Nayak, A K Abdul Hakeem, B Ganga, M Ijaz Khan, M Waqas and O D Makinde, *Comput. Meth. Prog. Biol.* **186**, 105131 (2020), https://doi.org/10.1016/j.cmpb.2019.105131

[12] W A Khan, I Haq, M Ali, M Shahzad, M Khan and M Irfan, *J. Braz. Soc. Mech. Sci. Eng.* **40**, 470 (2018), https://doi.org/10.1007/s40430-018-1390-3

[13] W A Khan, M Ali, F Sultan, M Shahzad, M Khan and M Irfan, *Pramana – J. Phys.* **92**, 16 (2019), https://doi.org/10.1007/s12043-018-1678-y

[14] S Muhammad, G Ali, S I A Shah, M Irfan, W A Khan, M Ali and F Sultan, *Pramana – J. Phys.* **93**, 40 (2019), https://doi.org/10.1007/s12043-019-1800-9

[15] B Ganga, S Mohamed Yusuff Ansari, N Vishnu Ganesh and A K Abdul Hakeem, *J. Taibah Uni. Sci.* **11(6)**, 1200 (2017)

[16] B Ganga, S Mohamed Yusuff Ansari, N Vishnu Ganesh and A K Abdul Hakeem, *Propuls. Power Res.* **5**(**3**), 211 (2016)

[17] M Shahzad, M Ali, F Sultan, W A Khan and Z Hussain, *Indian J. Phys.* **95**, 481 (2021), https://doi.org/10.1007/s12648-019-01669-3

[18] Z Hussain, R Zeesahan, M Shahzad, M Ali, F Sultan, A M Anter, H Zhang and N Khan. *Pramana – J. Phys.* **95**, 27 (2021), https://doi.org/10.1007/s12043-020-02043-3

[19] Z Hussain, M Ali, M Shahzad and F Sultan, *Pramana – J. Phys.* **94**, 49 (2020), https://doi.org/10.1007/s12043-019-1900-6

[20] Z Hussain, A ur Rehman, A J Shaikh, K Hu, M Ali, F Sultan, M Shahzad and M Altanji, *Case Stud. Therm. Eng.* **26**, 100998 (2021), https://doi.org/10.1016/j.csite.2021.100998

[21] A K Abdul Hakeem, M Govindaraju and B Ganga, *J. Heat Mass Transf. Res.* **6**(**1**), 1 (2019)

[22] M Shahzad, F Sultan, I Haq, M Ali and W A Khan, *Pramana – J. Phys.* **92**, 64 (2019), https://doi.org/10.1007/s12043

[23] W A Khan, H Sun, M Shahzad, M Ali, F Sultan and M Irfan, *Indian J. Phys.* **95**, 89 (2021), https://doi.org/10.1007/s12648-019-01678-2

[24] M Ali, F Sultan, M Shahzad and W A Khan, *Indian J. Phys.* **95**, 315 (2021), https://doi.org/10.1007/s12648-020-01706-6

[25] M Alghamdi, A Wakif, T Thumma, U Khan, D Baleanu and G Rasool, *Case Stud. Therm. Eng.* **28**, 101428 (2021), https://doi.org/10.1016/j.csite.2021.101428

[26] U Khan, A Zaib, I Khan and K S Nisar, *Int. Commun. Heat Mass Transf.* **127**, 105415 (2021), https://doi.org/10.1016/j.icheatmasstransfer.2021.105415

[27] K Sharma, *Pramana – J. Phys.* **95**, 113 (2021), https://doi.org/10.1007/s12043-021-02136-7

[28] Y Chu, U Khan, A Shafiq and A Zaib, *Arab. J. Sci. Eng.* **46**, 2413 (2021), https://doi.org/10.1007/s13369-020-05106-0

[29] M Waqas, A Alsaedi, S A Shehzad, T Hayat and S Asghar, *J. Braz. Soc. Mech. Sci. Eng.* **39**, 3005 (2017), https://doi.org/10.1007/s40430-017-0743-7

[30] T Hayat, Z Hussain, M Farooq, A Alsaedi and M Obaid, *Int. J. Nonlinear Sci. Numer. Simul.* **15**, 77 (2014)